






Experimental investigation on the relevance of mechanical properties and porosity of sandstone after hydrochemical erosion

CAI Yan-yan^{1*}  <http://orcid.org/0000-0001-5884-5952>;  e-mail: yycai@hqu.edu.cn

YU Jin¹  <http://orcid.org/0000-0003-0088-7652>; e-mail: buguayu0717@163.com

FU Guo-feng¹  <http://orcid.org/0000-0002-2945-5442>; e-mail: fugfen@126.com

LI Hong²  <http://orcid.org/0000-0002-7614-3484>; e-mail: hong.li@dlut.edu.cn

*Corresponding author

¹ Fujian Research Center for Tunneling and Urban Underground Space Engineering, Huaqiao University, Xiamen361021, China

² School of Civil and Hydraulic Engineering, Dalian University of Technology, Dalian116024, China

Citation: Cai YY, Yu J, Fu GF, et al. (2016) Experimental investigation on the relevance of mechanical properties and porosity of sandstone after hydrochemical erosion. Journal of Mountain Science 13(11). DOI: 10.1007/s11629-016-4007-2

© Science Press and Institute of Mountain Hazards and Environment, CAS and Springer-Verlag Berlin Heidelberg 2016

Abstract: Under the effect of chemical etching, the macroscopic mechanical properties, mesoscopic structure, mineral content, and porosity of rocks undergo significant changes, which can lead to the geological disasters; thus, an understanding of changes in the microscopic and macroscopic structure of rocks after chemical etching is crucial. In this study, uniaxial mechanical tests and nuclear magnetic resonance (NMR) spectroscopy were carried out on sandstone samples that had been previously subjected to chemical erosion under different pH values. The aim was to study changes in properties and mechanical characteristics, including deformation and strength characteristics, of the rock, and microscopic pore variation characteristics, and to perform preliminary studies of the chemical corrosion mechanism. Results show that different chemical solutions have a significant influence on the uniaxial compressive strength, the axial strain corresponding to the peak axial stress, elastic modulus, etc. With the passage of time, porosity increases gradually with exposure to different chemical solutions, and exposure to chemical solutions results in large changes in the NMR T2 curve and T2 spectrum area.

Received: 22 April 2016

Accepted: 28 June 2016

Sandstone exposed to different chemical solutions exhibits different corrosion mechanisms; the root cause is the change of mineral.

Keywords: Chemical erosion; Hydrochemistry; Mechanical properties; Nuclear magnetic resonance; Porosity; Sandstone

Introduction

Rock is always in a certain environment. Its mechanical properties will change by different degrees under the influence of various factors. The presence of water is a significant factor that affects the mechanical characteristics of rock (Ivars 2006; Zhang et al. 2010; Alonso et al. 2013; Dehkhoda and Hood 2014; Abdelghani et al. 2015). Soft rock in contact with water will become weaker (Li et al. 2015). In underground storage applications, such as CO₂ storage (Alonso et al. 2012) and groundwater reservoirs (Felice et al. 2014), it is necessary to consider the effect of water and ground stresses. Different water contents in rocks

will produce different freeze-thaw effects (Kodama et al. 2013). Thus, an understanding of the influence of water on rock is of crucial importance. In many water-related engineering constructions, such as underground storage and slope and dam foundation, the rock is affected not only by water, but also by the corresponding chemical solution (Eaton et al. 2007; Fantong et al. 2015), the mineral chemistry of the rock (Iler 1979; Atkinson and Meredith 1981; Ojala 2003; Moore et al. 2009), and the fracture mechanisms under chemical corrosion (Hu et al. 2012; Feng 2007). There has been a great deal of research on the subject. Grgic et al. (2014) has explored the influence of chemical solutions (water, oil, alcohol) on the acoustic emission and mechanical properties of porous rock, and demonstrated that the accumulation of acoustic emission events effectively reproduced the shape of the creep curve. Static elastic properties are important in revealing the creep characteristics of microcracks. Chai et al. (2014) observed the expansion effect of clayey rocks under exposure to different chemical solutions and concentrations and found that expansion and chemical solutions are unrelated but that expansion relies on the concentration of aqueous solutions: the higher the concentration, the weaker the expansion. Feng et al. (2009) investigated the mutual coupling effect of multiple cracks in limestone under exposure to different chemical solutions and uniaxial stresses and discovered that the influence of chemical etching is very complex. This influence depends on the concentration of chemical ions, pH value, mineral composition, geometry, number of defects, etc. Previous studies have indeed made some achievements, but have mainly focused on the macro and mesoscopic mechanical properties of rock and the distribution of cracks. However, the mineral impact on porosity under the action of aqueous solutions and the effect of changes of rock porosity on mechanical properties of rocks under chemical corrosion has not been well studied.

Sandstone is formed by deposition and diagenesis when sand is transported by water or glacier. It is a mineral aggregate formed by the cementation of all kinds of minerals and debris. In the process of diagenesis, the internal pore distribution of sandstone changes. Under the effect of chemical solutions, great changes have taken place in the pore size distribution of the internal

sandstone. Changes of porosity have caused macromechanical changes. Thus, it is very important to study porosity changes meticulously. Moreover, nuclear magnetic resonance (NMR) spectroscopy can study porosity changes in a meticulous and intensive manner (Xu 2011; Gao and Li 2015; Zargari et al. 2015). NMR spectroscopy has significant application value as a practical test, not only in such areas as medical diagnosis, agriculture, food, and polymer materials but also in the fields of geotechnical engineering, the mechanism of reservoir accumulation, oil and gas exploration and development, carbon sequestration, and investigations damages caused in rock mass (Schoenfelder et al. 2008; She and Yao 2010; Luo et al. 2011; Webber et al. 2013; Liu et al. 2014; Yao et al. 2014; Wang et al. 2015; Xiao et al. 2015). Therefore, it is significant to study the rock porosity change by using NMR spectroscopy, and to reveal the effect of porosity changes under water and chemistry interaction on macroscopic mechanical properties of rock and the relationship between these effects.

This study used uniaxial compression testing and NMR spectroscopy to investigate sandstone after treatment with different chemical solutions, to explore the influence of chemical solutions on porosity and mechanical properties and to determine the relationship between porosity change and degradation of mechanical properties. These results will reveal the root cause of changes to mechanical properties under the influence of different hydrochemical environments.

1 Materials and Methods

1.1 Sample preparation

The test material was sandstone cores, which were drilled from a single block without macroscopic cracks. The sandstone cores were machined into a cylindrical shape and were oriented vertical to the bedding plane with a diameter of 25 mm and a length of 50 mm. The heights (mean, 48.99 mm), diameters (mean, 24.91 mm), densities (mean, 2.42 g·cm⁻³) and masses (mean, 56.5 g) of the rock specimen are comparatively close to their mean values, which confirmed that the samples were almost uniform

and showed good homogeneity. Letters A, B, and C represent for acidic solution, neutral solution and alkaline solution respectively; numbers 12, 24, and 36 represent the number of days of immersion; and sample number 0 is the original sample.

1.2 Sample structure and mineral composition

The samples in this test are fragile-rigid arkose. The sandstone comes from a dam foundation, 5 meters below the surface, geological age is late Cenozoic, and it was saturated in-situ. Before the test, thin sections were prepared for identification and mineral composition identification using X-rays diffraction (XRD) analysis. The scientific name of the rock was fine-medium arkose, and the mineral composition of this rock was identified as fine-medium sand structure, contact cemented fine-grained sand pore type structure, and layered structure. The rock is composed of clasts (94%) and accessory minerals (1%), with cement (5%). Clasts of sandstone were semi-angular and semi-rounded, particle size 0.06–0.8 mm. Particles of 0.5–0.8 mm accounted for about 10%, particles of 0.25–0.5 mm about 50% and particles of 0.06–0.25 mm about 40%. Clastic composition is mainly feldspar and quartz, with a few hornblende, pyroxene, andesite grains. There is relatively less cement, which is mainly ferric oxide (2%) and carbonate (3%). The microscopic structure of the sandstone is shown in Figure 1.

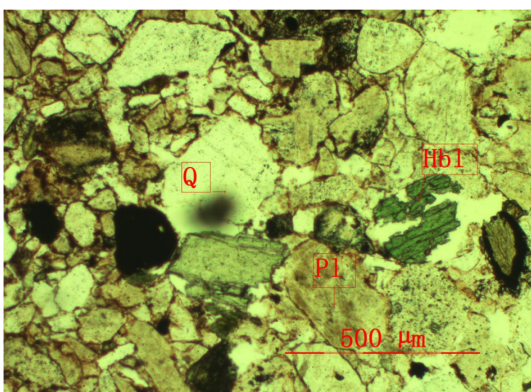


Figure 1 Microscope image of sandstone sample: Q, quartz; P1, plagioclase; Hb1, hornblende.

1.3 Test program

Engineering rock mass is always surrounded

by water, often containing complex ionic composition and varying pH values. This results from complex geological structure movement, as well as the dissolution of rock minerals and even environmental pollution. Because of the complexity of the ion composition and the influence of pH, the effect that the solution has on the rocks tends to be complex. To simplify the experimental study, the complex ionic composition was replaced by a simple NaCl solution. Acidic, neutral, and alkaline environments were simulated by pH values 2, 7, and 12, respectively. All initial concentrations of aqueous solutions were 0.01 mol·L⁻¹ with NaCl. To form the acid and alkali solutions, HNO₃ and NaOH, respectively, were added in aqueous solution. To balance the total number of ions, the same amount of NaCl was added into the neutral solution.

The sandstone samples were dried for 48 h at a constant temperature of 50°C, and samples with similar initial porosity were selected. The samples were saturated using a vacuum saturation device (Shanghai Niumag Corporation Ltd, China). After the pumping time and pressure are set, the equipment runs automatically; the pressure was set at 0.1 MPa. After saturation, samples were immersed in the acid, alkaline, and neutral solution for the required immersion times. After this, NMR spectroscopy was conducted, followed by a saturated uniaxial compression test. The mechanical test was conducted in a TAW-1000 servo-controlled rock mechanical test system (Figure 2). A strain control mode was used for loading, at a rate of 0.04 mm·min⁻¹, until the sample ruptured. Photographs to illustrate the failure mode after the test were taken.

The NMR spectroscopy (see Figure 3) was conducted using a MesoMR23-060H-I imaging analysis system (Shanghai Niumag Corporation Ltd, China). The permanent magnet magnetic field intensity is 0.52 T, the effective test area is 60 mm × 60 mm.

2 Results of Mechanical Experiments

2.1 Stress–strain relationship

Uniaxial compression testing of sandstone was carried out after immersion in different solutions

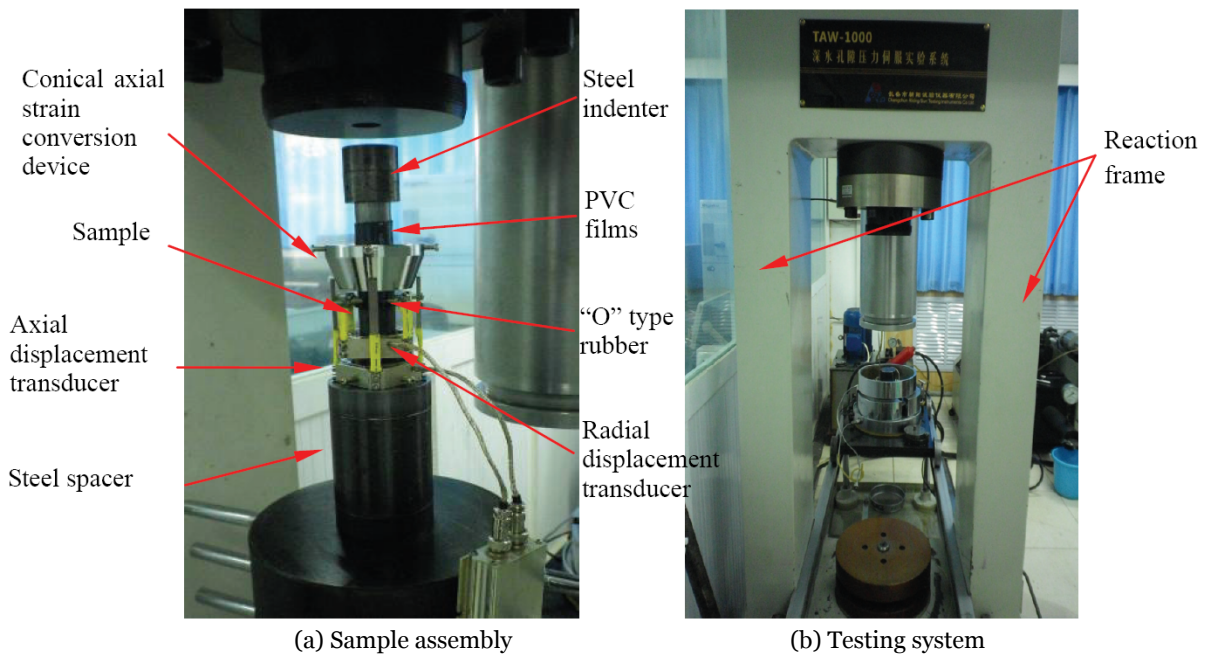


Figure 2 TAW-1000 servo-controlled rock mechanical test system.

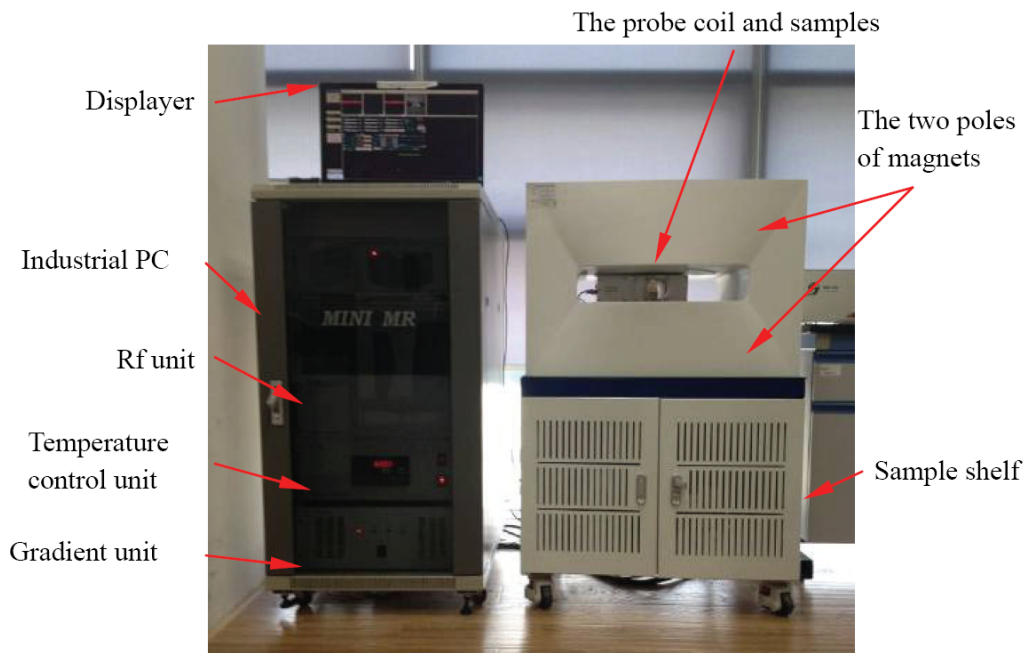
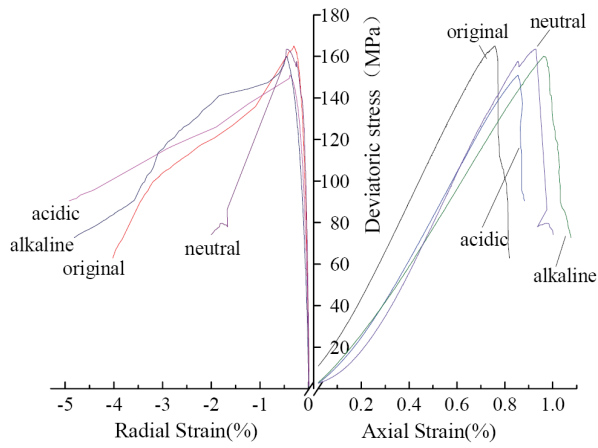


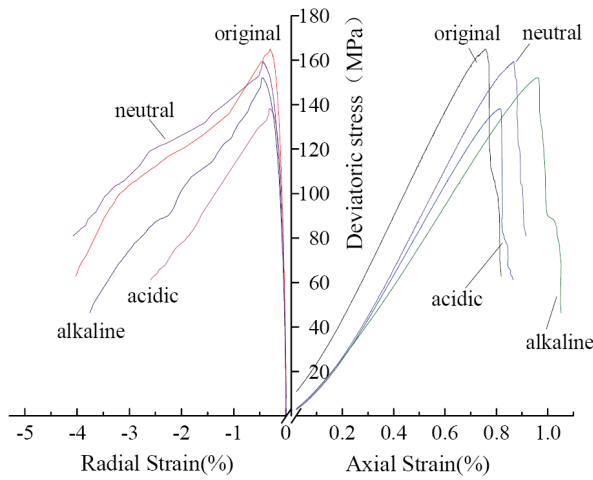
Figure 3 MesoMR23-060H-I type of NMR imaging analysis system.

for different time periods. The relationship between stress and strain after corrosion in different aqueous solutions can be seen in Figure 4. Figure 4 shows the uniaxial compression curves after the corrosion of sandstone in different chemical solutions. All the curves demonstrate compaction, elasticity, plasticity and a yield stage after a peak stress. Sandstone has a relatively high

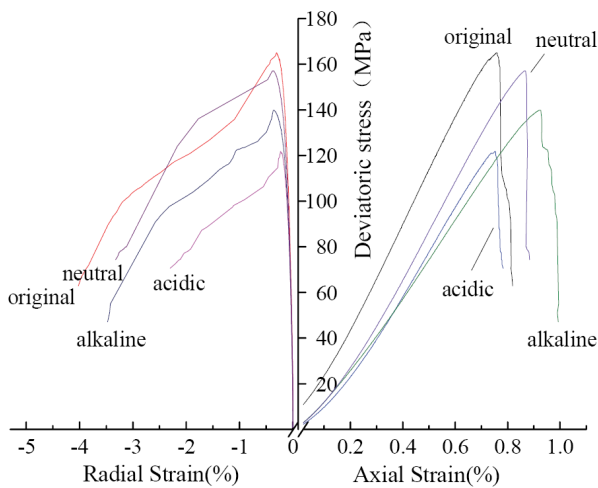
strength. The strengths of the original samples are up to 165.093 MPa. All the stress–strain curves of samples show obvious brittle characteristics. The strains in compaction stage for the samples immersed in different chemical solution are all high. Compared with samples immersed in neutral and acid solutions, the sample immersed in alkaline solution shows more significant



(a) 12 days



(b) 24 days



(c) 36 days

Figure 4 Stress strain curves of sandstone in different chemical solutions.

development in the stress–strain curve after the peak stage. Table 1 gives basic mechanical parameters of the samples, such as peak stress and peak strain.

Table 1 Sample physical parameters

Solution	Days	Ps (MPa)	Pas (%)	Prs (%)	E (GPa)	Poisson's ratio
Original	0	165.10	0.76	0.31	23.30	0.26
	12	150.93	0.86	0.41	20.72	0.25
Acid	24	138.21	0.81	0.37	20.11	0.24
	36	121.74	0.75	0.21	19.25	0.23
	12	163.54	0.93	0.45	22.74	0.26
Neutral	24	159.45	0.87	0.41	21.53	0.25
	36	157.14	0.87	0.38	21.43	0.24
	12	160.02	0.96	0.45	17.86	0.25
Alkaline	24	152.12	0.96	0.45	16.79	0.25
	36	139.84	0.92	0.36	15.82	0.23

Notes: Ps = Peak strength; Pas = Peak axial strain; Prs = Peak radial strain.

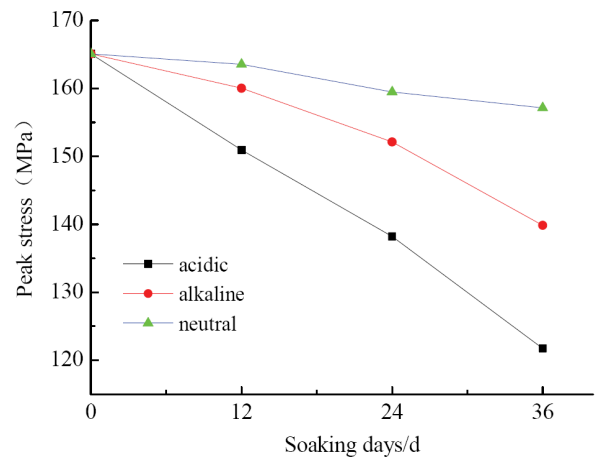


Figure 5 Peak stress of sandstone was soaked in different days under chemical solutions.

2.2 Peak strength

Figure 5 shows that the peak stress of sandstone varies with immersion time. It can be seen from Figure 4 that the peak strength of the sample immersed in neutral solution is always higher than that of the sample immersed in alkaline solution for the same length of time, and that the peak strength of the sample immersed in the acid solution is always a minimum. This is because the decrease in strength of sandstone exposed to a neutral environment is mainly caused by the softening of the rock that is immersed in water for a long time; there has not been a more violent chemical reaction. In acidic and alkaline environments, the chemical reaction is mainly between the mineral composition of rocks and H⁺ or OH⁻ ions in the solution. Figure 5 also shows that the reduction in peak strength in an acidic

environment is greater than that in an alkaline environment, indicating that, in acidic and alkaline solutions, there is a significant difference in the chemical corrosion mechanism of sandstone. Comparing this finding with the information in Figure 4, it can be seen that the strength of the sandstone soaked in neutral solution is only slightly reduced, compared with the strength of the natural sandstone. The peak stress of sandstone immersed in acidic solution is about 26.3% less than natural sandstone. The peak stress of sandstone immersed in alkaline solution is about 15.3% less than natural sandstone. After immersion in acidic or alkaline solutions, the strength of the sandstone is less than that of natural sandstone.

2.3 The axial peak strain

Figure 6 shows the peak axial strain of sandstone samples (which means the axial strain corresponding to peak stress) immersed in different chemical solutions for different time periods. The axial peak strain of sandstone samples immersed in different chemical solutions for 12 days has increased. This indicates that once the sandstone contacts the chemical solution, a series of chemical corrosions and dissolutions occur. In a neutral solution, this is mainly partial mineral dissolution. Chemical reactions with minerals mainly occur in the acidic and alkaline solutions. Chemical corrosion and dissolution both lead to an increase in porosity. Therefore, the peak axial strain increases. With the increase in immersion time, the peak axial strains of samples immersed in different chemical solutions are reduced by different amounts. This is because the chemical etching in the first 12 days is relatively fierce. With an increase in immersion time, the chemical reaction rates in solution have largely reduced, but at this stage the porosity has increased, so that the contact area between rock and chemical solution has increased. Thus, the chemical solution penetrates the rock more deeply, and at this stage the strength attenuation is still fast. Therefore, the peak axial strain decreases gradually. After the sandstone had been immersed for 36 days, the peak axial strain of the sample immersed in acid solution was reduced, but that of the sample immersed in neutral solution, did not change much. However, the peak axial strain of the sample

immersed in alkaline solution was increased.

2.4 Elastic modulus

Figure 7 shows the elastic modulus of sandstone samples immersed in different chemical solutions for different periods. With an increase in immersion time, the elastic modulus gradually decreased. The change in elastic modulus was smallest for the sample immersed in a neutral solution and largest for the sample immersed in an alkaline environment. The decrease in elastic modulus after the first 12 days of immersion is larger than that in the second 12 days. This is because in a neutral environment the reduction in sandstone strength is mainly due to the weakening of structure caused by the rock softening. In an alkaline environment, some minerals in the

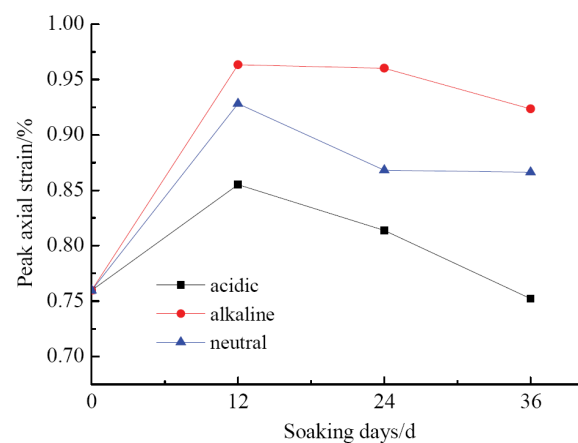


Figure 6 Peak axial strain of sandstone was soaked in different days under chemical solutions.

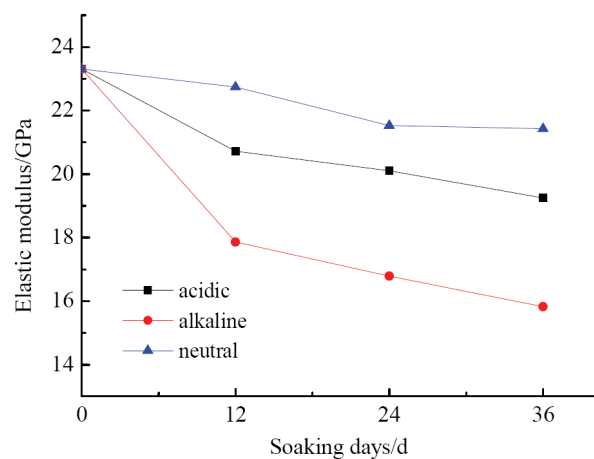


Figure 7 Elastic modulus of sandstone was soaked in different days under chemical solutions.

sandstone, such as feldspar and quartz, react with OH⁻ ions in solution. In an acidic environment, the rock strength decreases because some minerals, such as feldspar and calcite, react with H⁺ ions in solution, weakening the rock structure. The elastic modulus of original sandstone is 23.305 GPa. After the sandstone was soaked in acid solution for 36 days, the modulus of elasticity decreased to 19.247 GPa. The elasticity modulus of the sandstone immersed in neutral solution for 36 days is 21.426 GPa, which is only slightly less than that of the original sandstone. The elastic modulus of the sandstone sample immersed in alkaline solution for 36 days decreased significantly, to 15.824 GPa. This may be related to the main chemical components of SiO₂ in sandstone, which react with OH⁻ ions in alkaline environment.

2.5 Peak radial strain and Poisson’s ratio

Table 1 also shows that the peak radial strain of the sandstone samples immersed in different chemical solutions for 12 days increased. With an increase in immersion time, the peak radial strain in different chemical solutions reduced, by different amounts. From Table 1, it can also be seen that the Poisson’s ratio had no effect, which is why the variation in peak radial strain followed the same pattern as the peak axial strain.

2.6 Strain–volumetric strain curves in different solution

Martin et al. (1993) first proposed the crack strain model, to calculate crack initiation strength; this model soon found many applications (Eberhardt et al. 1999; Everitt et al. 2004). In the stress–strain relation shown in Figure 8, σ_{cc} is the crack closure stress level, σ_{ci} the crack initiation stress level, and σ_{cd} the crack damage stress level, which corresponds to the long-

term rock strength. The peak strength, σ_f , depends on the loading rate and boundary conditions. The four stress levels, i.e., σ_{cc} , σ_{ci} , σ_{cd} , and σ_f , represent important stages in the development of the microscopic crack in the rock. This study used the crack strain model to calculate the volumetric strain and the crack volumetric strain, as follows:

$$\epsilon_v = \frac{\Delta V}{V} = \epsilon_{axial} + 2\epsilon_{lateral} \tag{1}$$

$$\epsilon_{ve} = \frac{\Delta V}{V_{elastic}} = \frac{1-2\nu}{E}(\sigma_1+2\sigma_3) \tag{2}$$

$$\epsilon_{vc} = \epsilon_v - \epsilon_{ve} \tag{3}$$

where ϵ_v is the volumetric strain, ϵ_{axial} is the axial strain, $\epsilon_{lateral}$ is the lateral strain, ϵ_{ve} is the elastic volumetric strain, ΔV is the volume change, $V_{elastic}$ is the elastic volume, and ϵ_{vc} is the crack volumetric strain.

Figure 8 shows the axial and lateral strain of sandstone as well as the volumetric and crack volumetric strain, as calculated from Formula 3. The variation patterns of all the sandstone samples after immersion in different solutions for different

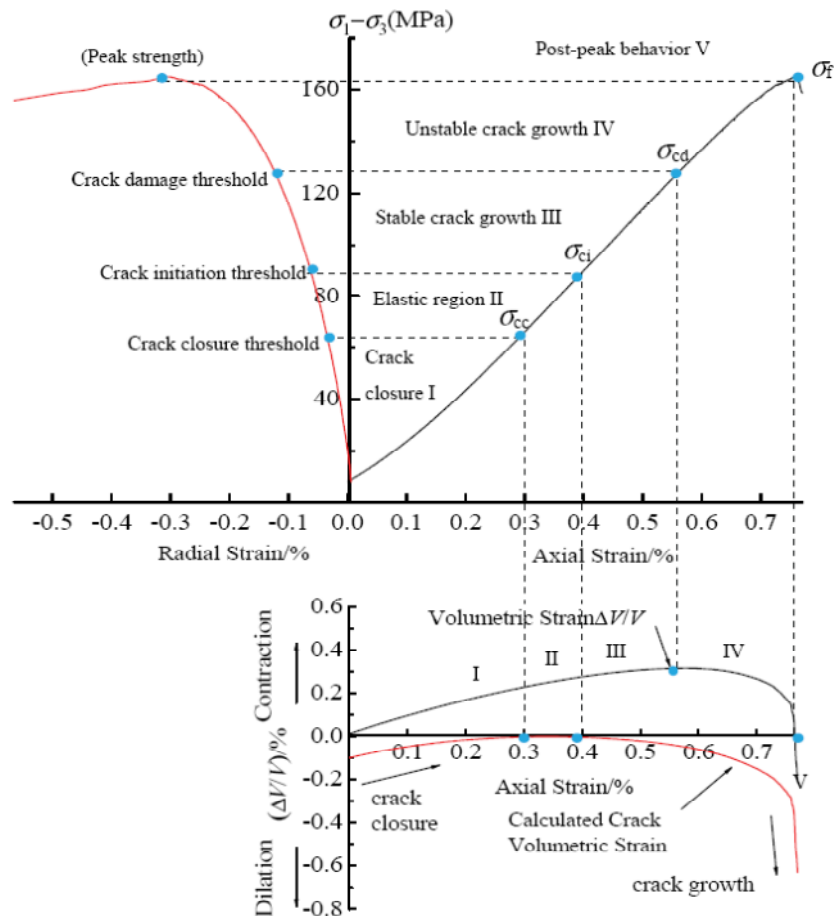


Figure 8 Stress-strain relationship after soaking in the solution.

periods are similar, so only the original sample is shown (related data are given in Table 2). Table 2 shows stress thresholds of the specimens, as determined by uniaxial compressive testing and their ratios under different conditions. Figure 8 and Table 2 demonstrate the following:

1) During the initial stage of the deviatoric experiment (stage I, non-linear elastic deformation), the material is compacted. With an increase of immersion time, σ_{cc} increases while σ_f decreases in different solutions, and σ_{cc}/σ_f increases gradually. It can be seen that in stage I, part of the stress-strain curve increases with an increase in immersion time; this is because some of the rock composition is lost and there is an increase in porosity.

2) The rock continues to become compressed with increasing axial loading (stage II, linear elastic deformation); at this stage, the crack volumetric strain remains constant. With an increase in immersion time, σ_{ci}/σ_f increases for immersion in different solutions, but the crack initiation stress σ_{ci} is not related to cyclic damage (Martin et al. 1994).

3) As loading continues to increase (stage III, volume strain comes to a minimum), the crack volumetric strain simultaneously begins to increase, and the microcrack population starts increasing. In acid and alkaline solutions, σ_{cd}/σ_f increases with an increase in immersion time. However, the value of σ_{cd}/σ_f does not change much for samples immersed in a neutral solution; this is because σ_{cd} is closely related to the cyclic damage increase, and when sandstone is only immersed in water, the mechanical properties are not much changed. The value of σ_{ci}/σ_{cd} increases with an increase in immersion time for different solutions; this is

because there is an increase in the initial damage, so crack propagation is reduced in stage III (Martin et al. 1994).

4) Before the stress reduction (stage IV, before the macroscopic failure), there is an obvious but gradual increase in crack volumetric strain, which might be linked to a higher number of microcracks.

5) As the loading is reduced (stage V, post-macroscopic failure), volumetric expansion begins. The crack volumetric strain reduces; this is probably because the cracks have become connected and irregular macrofractures have formed.

Figure 9 shows the crack volumetric strain of sandstone after immersion in different solutions for different periods. Figure 9 and Table 2 show that:

1) The value of volumetric strain corresponds to the compression phase of the original sample; $(\Delta V/V)_o$ is a minimum. The crack growth is most obvious in stages III and IV, the samples clearly exhibit brittle characteristics. The value of $(\Delta V/V)_o$ increases on immersion in different solutions; crack growth slows and the brittle behaviour is weakened.

2) The value of volumetric strain corresponds to the uniaxial peak intensity of rock; $(\Delta V/V)_f$ decreases for longer immersion periods in acid solution but gradually increases on immersion in alkaline solution. This is because the initial damage leads to an increase in damage with increased immersion times in acid solution. Because the initial amount of damage is higher, there is a relatively small amount of crack extension that could cause sample fracture. The rock shows a certain degree of improvement in mechanical

Table 2 Stress thresholds of specimen obtained by uniaxial compressive test and their ratios under different conditions

Solution	Days	ε_{cc} (%)	ε_{ci} (%)	$(\Delta V/V)_o$ (%)	$(\Delta V/V)_F$ (%)	σ_{cc} (Mpa)	σ_{ci} (Mpa)	σ_{cd} (Mpa)	σ_f (Mpa)	σ_{cc}/σ_f	σ_{ci}/σ_f	σ_{cd}/σ_f	σ_{ci}/σ_{cd}
Original	0	0.32	0.36	0.10	0.31	69.92	80.39	132.19	165.09	0.42	0.49	0.80	0.61
	12	0.32	0.37	0.16	0.49	46.00	54.65	108.08	150.93	0.30	0.36	0.72	0.51
Acid	24	0.37	0.42	0.14	0.43	56.51	68.09	105.09	138.21	0.41	0.49	0.76	0.65
	36	0.39	0.47	0.17	0.19	52.22	67.38	102.21	121.74	0.43	0.55	0.84	0.66
Neutral	12	0.34	0.35	0.19	0.12	46.15	58.34	130.11	163.54	0.28	0.36	0.80	0.45
	24	0.35	0.43	0.17	0.47	56.64	69.90	105.76	159.45	0.36	0.44	0.66	0.66
	36	0.41	0.46	0.16	0.46	58.79	72.67	113.64	157.14	0.37	0.46	0.72	0.64
	12	0.32	0.39	0.11	0.21	47.58	50.25	102.75	160.02	0.30	0.31	0.64	0.49
Alkaline	24	0.36	0.45	0.14	0.40	57.67	67.17	107.63	152.12	0.38	0.44	0.71	0.62
	36	0.39	0.50	0.14	0.41	59.50	66.29	111.54	139.85	0.43	0.47	0.80	0.59

properties in alkaline solution; the lateral strain is larger than that in the original sample, and the failure is more obvious.

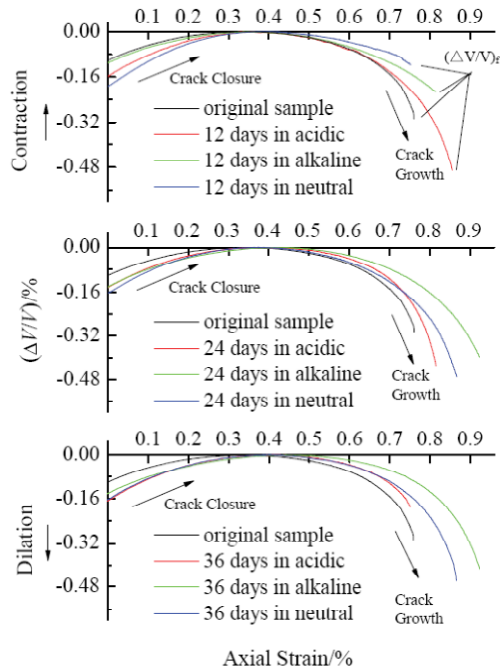


Figure 9 Crack volumetric strain of sandstone after soaking in different solutions in different days.

3) Both ϵ_{cc} and ϵ_{ci} increased with an increase in immersion time when fissures were closed completely, in the different solutions; this is because the porosity increased gradually.

It can be seen from the curvature of the crack volumetric strain curve in stages III and IV and from the value of crack volumetric strain for the same value of axial strain, that crack growth is quicker for exposure to acid solutions than for exposure to alkaline solutions.

2.7 Failure mode

The essence of rock failure is that the accumulation of damage in the process of loading reached the maximum damage point that the rock could bear, and macroscopic rupture occurred as a result. This is the macroscopic embodiment of microscopic fissure accumulation. Figure 10 shows a sample of rock after chemical etching. At this point, the sample is still whole because it still has some residual strength. The figure shows that the failure characteristics of specimens under uniaxial compression are basically similar after different

types of chemical corrosion. In each case, the failure mode is splitting. The crack propagation direction and the loading direction are parallel or at a small angle to each other. The number of cracks is relatively higher and the cracks are connected. At the end of the sample, has fall-block, while the middle part of the sample has the crack perpendicular to the loading direction. From these results, it can be seen that the failure mode of the sandstone immersed in the different solutions was not fundamentally changed as a result of the increase in porosity. Crack initiation and extension from the sample end form several main macroscopic cracks, leading to fracturing. The fracturing occurred very quickly, but the sample still held its cylindrical shape. When an external

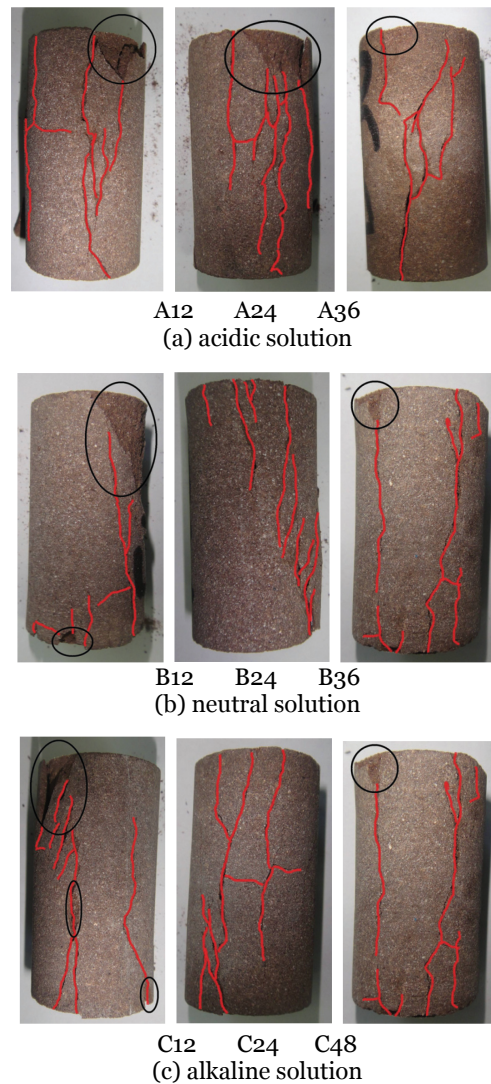


Figure 10 Rock failure pictures after chemical etching.

force is applied, the sample will lose residual strength and disintegrate along the crack directions.

3 Results of NMR Experiments

3.1 Porosity

The results of the mechanical tests reveal that sandstone undergoes different chemical reactions in different solutions. Moreover, owing to the different chemical corrosion mechanisms, a series of changes take place, which affect such macroscopic mechanical parameters as peak stress and elastic modulus. The root cause is that the change in porosity after immersion in the solutions. Therefore, the porosity of sandstone samples immersed in different solutions was investigated using NMR spectroscopy. The results are shown in Table 3 and Figure 11. The void space in the rock is comprised of micro-cracks and pores. Before uniaxial compression testing, most of the void space would be pores, only a small part of void space is micro-cracks, so the porosity is comprised of micro-cracks and pores.

Table 3 and Figure 11 show that with the increase in immersion time, the porosity increased. However, the increase rate varied with immersion in different solutions. Because the porosity of the sample was selected before immersion, there were only small differences in the initial porosities of the samples. The porosities varied between 5.86% and 5.98%, with a mean of 5.89%. After immersion, the porosity increased by different amounts. Samples immersed in acidic solution for 36 days, showed a porosity increase of 29.98%. For the same immersing period, the porosity of samples immersed in alkaline solution increased by 18.51%. The samples immersed in neutral solution showed the smallest increase in porosity; 10.07%. Therefore, the most intense chemical reaction occurred in the acid solution, and the least in the neutral solution. Table 3 also shows a clear change in porosity for samples immersed in the different solutions for 12 days. The rate of increase in porosity decreases with increasing immersion time. For example, in a neutral environment, the sandstone sample immersed for 12 days showed a 6.02% increase in porosity. After a further 12 days immersion, the porosity increase by only a further

2.26%. When the sandstone sample had been immersed for a total of 36 days the porosity increased by a further 1.79% compared to that of the porosity after 24 days' immersion. Similarly, the rate of the porosity increase for immersion in acid and alkaline environments decreased with an increase in immersion time. This is because, in the chemical environment, at first there are more internal mineral particles reacting or being dissolved. With the passage of time, the amount of dissolved and reactive minerals in sandstone has gradually reduced, and the ion concentration has increased; that is, the concentrations of H⁺ in the acid solution and OH⁻ in the alkaline solution keep reducing and the pH of the solution tends towards neutral. At the same time, the chemical solution penetrates the rock interior more deeply and the number of reactive substances is further reduced. Therefore, the rate of porosity increase is reduced.

Table 3 Rock porosity and its percentage change

Sample No.	PH value	Original porosity (%)	Corrosion porosity(%)	Percentage change(%)
0	-	5.89	5.89	0.00
A12	2	5.95	6.92	16.30
A24	2	5.88	7.28	23.81
A36	2	5.87	7.63	29.98
B12	7	5.98	6.34	6.02
B24	7	5.92	6.41	8.28
B36	7	5.86	6.45	10.07
C12	12	5.90	6.61	12.03
C24	12	5.93	6.82	15.01
C36	12	5.89	6.98	18.51

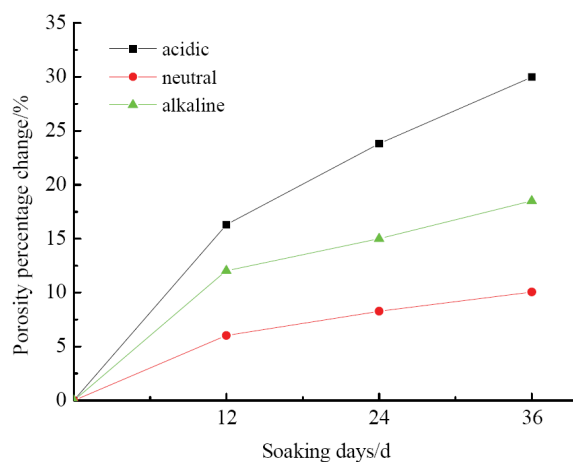


Figure 11 Porosity percentage change of sandstone in different chemical solutions after different days soaking.

3.2 NMR T2 spectrum distribution

The core technology of NMR spectroscopy utilizes atomic nuclear spin characteristics and the attenuation signal produced by polarization in a static magnetic field. Among these, T2 is the decay time for the transverse magnetization vector. The measured signal for rock fully immersed in water can be interpreted as a measure of the volume of water in the rock, which is the pore volume. The smaller the pore volume is, the shorter the relaxation time. The peak position of the T2 curve illustrates the pore size, and the area of the peak is related to the quantity of corresponding pores. The ratio of the area below the peak to the whole area represents the percentage of the corresponding pore size to the total porosity, and the T2 spectrum indicates the pore size distribution.

Figure 12 shows the T2 spectrum and magnetic resonance imaging (MRI) scans of sandstone immersed in original and different chemical solutions for different periods. The T2 spectrum distribution for sandstone in the natural state has one peak. The NMR spectrum has a maximum at 0.215 ms, which corresponds to a pore size of 0.02–0.03 μm, indicating that the sample has a large number of medium and tiny pores. After the strongest peak, at increasing relaxation times, the pore size increases and the number of pores of these sizes decreases gradually. After sandstone has been immersed in different chemical solutions for 12 days, changes in porosity can be observed. The T2 spectrum has changed not only in an increase in total pore content, but also in curve

shape. After immersing the sandstone in different solutions, the largest NMR peak has increased in signal strength. The increasing signal intensity of the T2 peak at 10 ms, corresponding to an aperture size of 1 μm, indicates an increase in pores of this size. In addition, there are now two peaks in the spectrum. For the samples immersed in a neutral solution, the number of small pores increases, and the medium-sized pores expand. This is because, with immersion in water, some of the minerals in the sandstone dissolve, leading to the formation of small pores, and to the enlargement of these pores. Furthermore, the dissolution of minerals between pores has caused small pores to be combined to form larger pores. Under acidic conditions, the number of small pores appears to be greatly increased, and the number of large pores is also significantly increased. Therefore, the total porosity is increased. This is because some of the rock clasts, such as feldspar, react with acids and the cementing material is easily dissolved in an acidic solution. When these reactive minerals are isolated by minerals that do not react easily, small pores are easily formed. When isolated by reactive minerals, the pore size will expand and the number of large pores will increase. In alkaline environments, the changes in the porosity are roughly similar to those observed in acidic conditions. The number of small pores and big pores has significantly increased. This is because rock clasts such as quartz and feldspar react with alkalis, causing obvious chemical injury.

Magnetic resonance imaging (MRI) was performed on sandstone samples after immersion

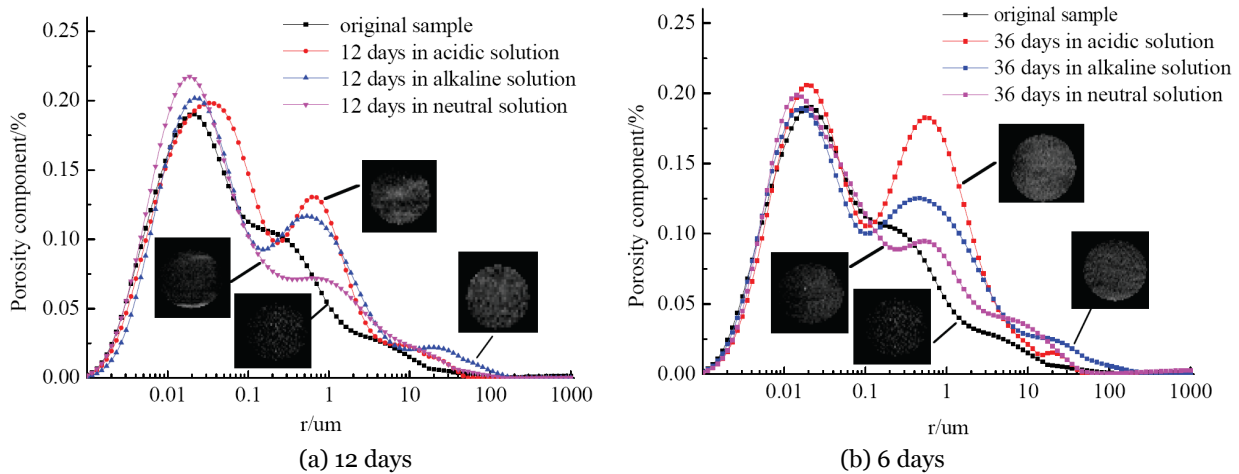


Figure 12 T2 spectrum distribution of sandstone in original and different chemical solutions after different days soaking.

for different periods; using central sample cross-section 2-dimensional imaging. Bright areas in the image area correspond to water molecules; the black surround area around is the background. The brightness of the image reflects the moisture content of the rock; the brighter the color, the higher the water content, and so the higher the pore area. It can be seen from the diagram that the sample image of the natural sandstone is not clear. The images of samples taken after immersion in different solutions shows increasing water content; the brightness of the image obtained after immersion in 12 days in the acid or alkaline solutions is significantly higher than that of the image obtained for the sample immersed in a neutral environment for the same period.

Figure 12(b) shows that, for the samples immersed in solution for 36 days, there was no obvious change in porosity component at 0.02–0.03 μm, compared with data for the samples immersed for 12 days. However, there is a porosity component at 1 μm, that is, there is a clear increase in the amplitude of the second peak, especially under acidic conditions. This is because when the number of 0.02–0.03 μm pores increases, some of these pores become interconnected, forming larger pores. The figure also shows that the pore change observed in neutral salt solution is less obvious than that in alkaline environment, while it is most obvious in the acidic environment. This is because in different chemical solutions, the strength and influence of chemical reactions are different. With an increase in immersion time in chemical solution, rock damage is gradually intensified. In neutral salt solution, only a small proportion of the rock minerals dissolve in water to form new pores, as mineral dissolution is relatively weak. Therefore, in a neutral environment, the T2 spectrum is not much changed. The reaction taking place in acidic solution is strong, and more mineral types react with H⁻ ions. Furthermore, the reaction products are always in ion form. With an increase in immersion time, the acid solution continuously permeates the sandstone, forming new microscopic pores and expanding small pores. In alkaline solution, part of the minerals reacting with OH⁻ ions produce soluble ions, and the reaction also generates some refractory minerals. Therefore, chemical corrosion in acidic conditions increases porosity more than that in an alkaline environment.

It can be seen from the figure that, in the samples immersed for 36 days, water content has further increased, as the solutions have penetrated the sample more deeply, and the degree of corrosion in the samples is increased. This figure supports the mechanical test results, and is also in good agreement with the T2 spectrum and porosity.

3.3 NMR T2 spectrum area

The larger the porosity of the rock, the more fluid is contained inside the rock, and the larger the T2 spectrum area. Thus, the changes in rock porosity can be further analyzed by measuring the T2 spectrum area. The sandstone T2 spectrum area and proportional area for each peak are shown in Table 4.

Table 4 NMR spectrum area

Sample No.	Peak total area	Percentage of first peak(%)	Percentage of second peak (%)
0	5902	100	-
A12	7021	67.55	32.45
A36	8361	49.97	50.03
B12	6576	100	-
B36	6985	71.04	28.96
C12	7110	61.03	38.97
C36	7482	53.35	46.65

From Table 4, it can be seen that sandstone that is not immersed in solution had the smallest T2 spectrum area and only one T2 spectrum peak. When the rock was immersed in different chemical solutions, the T2 spectrum distribution changed; a second peak appeared and the T2 spectrum area increased. After immersion for 12 days in neutral solution, the T2 spectrum of sandstone still had only one peak. After 36 days immersion, a second peak is seen but the percentage is only 28.96%. Soaked in acidic and alkaline solutions for 36 days, respectively, the percentages of the second peak are 50.03% and 46.65%, higher than that observed for the sample immersed in the neutral environment. After the sandstone had been immersed in acidic and alkaline solutions for 12 days, the second peak of the T2 spectrum appeared. With an increase in immersion time, the percentage of the second peak increased. This is because minerals in the sandstone dissolve, clastic rock and cementation material undergo acid–base reactions, microscopic pores are formed and expand, as they become

interconnected. As larger pores are formed, the second peak appears and becomes stronger with an increase in etching time; as immersion time is increased, the proportion of the second peak is increased.

4 Chemical Corrosion Mechanism

4.1 Chemical damage

It is important to choose appropriate variables in studying chemical damage. The choice of variables can be made by adopting a macroscopic or a microscopic view. However, for the sandstone samples, which are corroded by chemical solution, the change of porosity is the root cause of changes in the rock's mechanical properties. Therefore, this study used porosity as a variable to reflect the degree of corrosion in different chemical solutions.

Chemical damage variables are calculated as:

$$D_t = 1 - \frac{1 - \phi_t}{1 - \phi_0} \quad (4)$$

where D_t is the damage variable after t days immersion, ϕ_0 is the porosity of the original sample, and ϕ_t is the porosity after immersion for t days.

Figure 13 shows a quadratic fitting equation between the damage variable and different immersion periods:

$$\begin{cases} D_a = 0.02507 + 0.09111t - 0.00113t^2 & \text{acidic} \\ D_b = 0.01065 + 0.03413t - 0.00048t^2 & \text{neutral} \\ D_c = 0.02507 + 0.09111t - 0.00094t^2 & \text{alkaline} \end{cases} \quad (5)$$

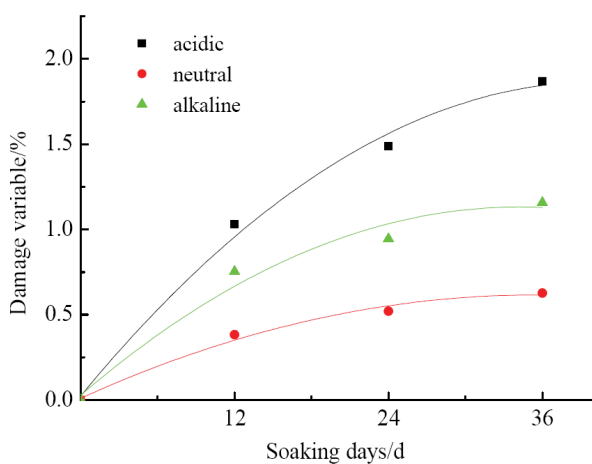


Figure 13 Damage variable of sandstone in different soaking days under chemical solutions.

Figure 13 and Formulas (5) illustrate that all the damage variables increase in different chemical solutions with an increase in immersion time, and that the rate of increase decreases gradually. The damage degree of sandstone in acidic solution is always greater than that in alkaline solution, and the degree of chemical corrosion is smallest in the neutral environment. This is because the number of minerals that can react and the concentration of H^+ and OH^- ions in the chemical solution are gradually reduced. Hence, the rate of reaction and growth rates of damage decreases.

4.2 Corrosion mechanism analysis

At a macroscopic level, the chemical damage has caused reductions in mechanical parameters to varying extents. Changes in macroscopic mechanical parameters are the result of changes in microscopic structure change, which are the root cause of degradation of macroscopic mechanical parameters degradation. This means that changes in macroscopic mechanical properties are closely related to changes in microstructure.

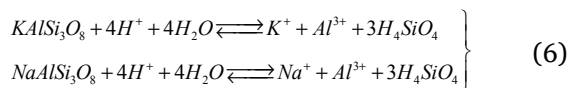
The microstructure change in composition and porosity of rock is the essence of hydrochemical corrosion. Several factors have contributed to changes in the composition and porosity of rock. First, there is dissolution. Water acts as a solvent, and cementitious minerals and some mineral particles in the rock in contact with water will dissolve and become diffused in the aqueous solution to a certain degree. This leads to an increase in porosity and softening of rock structure. Second, there is hydrolysis. Some cations in the mineral react easily with hydroxyl ions in chemical solution, forming new minerals. Finally, there is acid-base reaction, some minerals, such as calcite and dolomite in sandstone react easily with hydrogen ions in acid conditions.

Mineral compositions in different rocks are different, which means that chemical corrosion effects also differ. The fine grain arkose of this paper contains feldspar (71%), quartz (15%), andesite cuttings (4%), hornblende (2%), pyroxene (2%), accessory mineral (1%) and cement (5%); the main composition of the cement is calcite cement and iron oxide. The mineral components of sandstone are varied and their chemical actions differ. Some cations, such as K^+ , Na^+ , Ca^{2+} , and

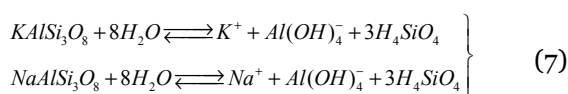
Mg²⁺ easily react with hydroxyl ions, to convert the original minerals into new minerals. Moreover, some of these mineral components, such as plagioclase, hornblende, and calcite, are soluble in water, causing secondary porosity, as well as changes in the rock structure, which cause the rock to become softer. Feldspar and quartz accounted for 86% of the total mineral content; therefore, although the cement mineral has an important influence on microstructure, the influence of feldspar and quartz is most important.

Feldspar will undergo a certain degree of dissolution and hydrolysis in the chemical environment. The difference between primary and secondary minerals is the formation of secondary porosity. In solutions with different pH values, the products of feldspar reactions will differ. Potassium feldspar and albite react in acid and alkaline solutions as follows.

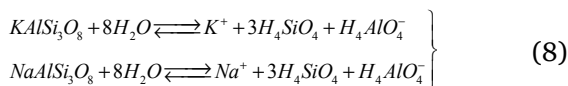
In acidic (pH < 6) conditions:



In neutral or alkaline (6 < pH < 10) conditions:

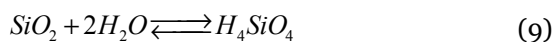


In strongly alkaline (pH > 10) conditions:

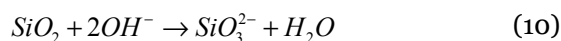


Formulas 6–8 show that the main components of arkose are more likely to react with different chemical solutions. Because of the reaction, the silicate rock has produced secondary porosity.

The main mineral composition of quartz is SiO₂, which is stable in acidic and neutral environments. The reaction in pure water is:

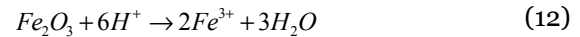
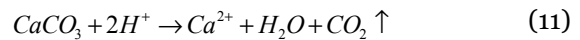


The reaction in alkaline solution is:



In addition, the content of cement minerals is small, but because the strength of cement minerals is often less than that of the mineral particles, the reactions of the cement minerals have a great influence on the mechanical properties of rock, thus the stability of cementing mineral in different chemical solution is particularly important. In this

study, the cementing minerals were mainly calcite and iron oxide. The following reactions are likely in acidic solution:



Calcite and iron oxide are both stable in neutral and alkaline environments. Other minerals, such as andesite cuttings, amphibole, and pyroxene are present in smaller quantities, and are relatively stable mineral particles.

Formulas (6)–(12) show that feldspar, as a main mineral of sandstone, undergoes different reactions in different chemical environments, resulting in various degrees of increasing porosity. Quartz is reactive in an alkaline environment. This is why sandstone porosity in alkaline environment is greater than that in a neutral environment. In addition, cementitious minerals can react with acid solutions, and the reaction of the cement mineral does not produce sediment, so the porosity is larger than that found in alkaline environments.

The porosity of sandstone in a chemical corrosive environment increases gradually, owing to the influence of dissolution, hydrolysis, and some chemical effects. At the same time, the solute concentration increases gradually. Where these reactions have taken place at the water–rock interface, the ion concentration in the pores increases, increasing the osmotic pressure in internal aqueous solution. Actuated by osmotic pressure, there is chemical etching more deeply inside the rock, and the amount of chemical damage increases with time. Since fewer cracks are produced by water chemistry corrosion, the change in rock porosity is almost all due to the effect of secondary porosity; thus, our analysis ignores the influence of fractures on mechanical parameters. This analysis supports the results of the porosity tests obtained by NMR spectroscopy, and the fact that the changes in porosity reflect changes in the sample’s macroscopic mechanical parameters.

5 Conclusions

This study investigated the evolution of the mechanical properties and porosity changes of sandstone in different chemical solutions, and

elucidated the effect of mineral changes in causing porosity change. Based on the data and analysis, the following conclusions can be made.

Sandstone has the highest peak strength of the original sample. After immersion in solutions, the strength of the rock is reduced; the largest reduction was for acid solutions, followed by alkaline and neutral solutions. The peak strength of sandstone decreases over time for immersion in different chemical solutions. At the beginning of chemical immersion, the peak axial strain of sandstone increases, but with the passage of time, the peak axial strain in different solutions are reduced by varying amounts. The elastic modulus decrease after chemical immersion, and the elastic modulus reduce with increasing immersion time. The elastic modulus of sandstone immersed in neutral solution is highest, and that immersed in alkaline solution is lowest; the modulus of sandstone immersed acidic solution is between these two values. The radial peak strain has almost the same trend as the axial peak strain; that is, Poisson's ratio has no effect and is constant.

In strain–volumetric strain curves, which could be divided into five stages, stage I lengthens with an increase in immersion time, and σ_{ci}/σ_f increases in different solutions, but the crack initiation stress σ_{ci} is not related with cyclic damage. With the initial damage increase, the crack propagation will decrease in stage III, and the rate of damage increase will be reduced when the volume of sandstone is restored to its original size in stage IV. In stage V, the volumetric dilation begins. The crack volumetric strain suddenly decreases. The value of volumetric strain $(\Delta V/V)_o$ corresponds to the compression phase of the original sample is a minimum, and $(\Delta V/V)_o$ increases for immersion in different solutions, while $(\Delta V/V)_f$ decreases in acid solution and gradually increases in alkaline solutions; ε_{cc} and ε_{ci} both increased in different solutions. In stages III and IV, the crack growth in acid solutions is quicker than that in alkaline solutions.

All uniaxial compression failure modes are splitting failure after chemical immersion. A large

number of longitudinal cracks are initiated. The propagation direction of the cracks is parallel to the loading direction or at a small angle. There is expansion at the central part of sample and cracks that run parallel to the end face.

When sandstone was immersed in different solution, porosity increased over time; the increase in porosity is greatest for immersion in acid solution, followed by alkaline and neutral solution; this trend corresponds with findings on peak strength. With increasing immersion time, the rate of increase in porosity reduced for all samples. In the NMR spectroscopy experiments, the T2 spectrum for the original sample of sandstone had only one peak, but a second peak emerged after the samples had been immersed in the solutions. As the immersion time increased, the intensity of the second peak increased, and the proportional area of the second peak also increased.

The amount of damage for sandstone immersed in acidic solution is always greater than that for sandstone immersed in an alkaline environment, and the degree of chemical corrosion is lowest in neutral environment. Feldspar will undergo a certain amount of dissolution and hydrolysis in a chemical environment. In solutions with different pH values, the products of feldspar reactions will be different. Quartz in alkaline solution will react. The proportion of cement minerals is small, but the cement has a great influence on the mechanical properties; cement minerals are reactive in acidic solutions.

Acknowledgements

This work was supported by the National Basic Research Program of China (973 Program) (Grant No. 2011CB013503), the National Natural Science Foundation of China (Grant No. 51374112, 51679093), and the Promotion Program for Young and Middle-aged Teacher in Science and Technology Research of Huaqiao University (ZQN-PY112, ZQN-PY311).

References

Ivars DM (2006) Water inflow into excavations in fractured

rock—a three-dimensional hydro-mechanical numerical study.

- International Journal of Rock Mechanics and Mining Sciences 43: 705-725. DOI: 10.1016/j.ijrmms.2005.11.009
- Zhang HB, Zhang W, Lv L, et al. (2010) Effect of fissure water on mechanical characteristics of rock mass. *Mining Science and Technology (China)* 20: 846-849. DOI: 10.1016/S1674-5264(09)60293-3
- Alonso EE, Zandarin MT, Olivelia S (2013) Joints in unsaturated rocks: thermo-hydro-mechanical formulation and constitutive behaviour. *Journal of Rock Mechanics and Geotechnical Engineering* 5: 200-213. DOI: 10.1016/j.jrmge.2013.05.004
- Dehkhoda S, Hood M (2014) The internal failure of rock samples subjected to pulsed water jet impacts. *International Journal of Rock Mechanics and Mining Sciences* 66: 91-96. DOI: 10.1016/j.ijrmms.2013.12.021
- Abdelghani FB, Aubertin M, Simon R, Therrien R (2015) Numerical simulations of water flow and contaminants transport near mining wastes disposed in a fractured rock mass. *International Journal of Mining Science and Technology* 25: 37-45. DOI: 10.1016/j.ijmst.2014.11.003
- Li GC, Jiang ZH, Lv CX, et al. (2015) Instability mechanism and control technology of soft rock roadway affected by mining and high confined water. *International Journal of Mining Science and Technology* 25: 573-580. DOI: 10.1016/j.ijmst.2015.05.009
- Alonso J, Navarro V, Calvo B, et al. (2012) Hydro-mechanical analysis of CO₂ storage in porous rocks using a critical state model. *International Journal of Rock Mechanics and Mining Sciences* 54:19-26. DOI: 10.1016/j.ijrmms.2012.05.016
- Felice SL, Montanari D, Battaglia S, et al. (2014) Fracture permeability and water-rock interaction in a shallow volcanic groundwater reservoir and the concern of its interaction with the deep geothermal reservoir of Mt. Amiata, Italy. *Journal of Volcanology and Geothermal Research* 284: 95-105. DOI: 10.1016/j.jvolgeores.2014.07.017
- Kodama J, Goto T, Fujii Y, et al. (2013) The effects of water content, temperature and loading rate on strength and failure process of frozen rocks. *International Journal of Rock Mechanics and Mining Sciences* 62: 1-13. DOI: 10.1016/j.ijrmms.2013.03.006
- Eaton TT, Anderson MP, Bradbury KR (2007) Fracture control of ground water flow and water chemistry in a rock aquitard. *Ground Water* 45:601-615. DOI: 10.1111/j.1745-6584.2007.00335.x
- Fantong WY, Kamtchueng BT, Yamaguchi K, et al. (2015) Characteristics of chemical weathering and water-rock interaction in Lake Nyos dam (Cameroon): Implications for vulnerability to failure and re-enforcement. *Journal of African Earth Sciences* 101:42-55. DOI: 10.1016/j.jafrearsci.2014.08.011
- Iler RK (1979) *The chemistry of silica: solubility, polymerization, colloid and surface properties, and biochemistry*. Wiley-Interscience Publication, New York. DOI: 10.1002/anie.198002302
- Atkinson BK, Meredith PG (1981) Stress corrosion cracking of quartz: a note on the influence of chemical environment. *Tectonophysics* 77(1-2): T1-T11. DOI: 10.1016/0040-1951(81)90157-8
- Ojala I, Ngwenya BT, Main IG, et al. (2003) Correlation of microseismic and chemical properties of brittle deformation in Lochaberbriggs sandstone. *Journal of Geophysics Research* 108 (B5): 2268. DOI: 10.1029/2002JB002277
- Moore KR, Wall F, Divaev FK, et al. (2009) Mingling of carbonate and silicate magmas under turbulent flow conditions: Evidence from rock textures and mineral chemistry in sub-volcanic carbonatite dykes, Chagatai, Uzbekistan. *Lithos* 110: 65-82. DOI: 10.1016/j.lithos.2008.11.013
- Hu DW, Zhou H, Hu QZ, et al. (2012) A hydro-mechanical-chemical coupling model for geomaterial with both mechanical and chemical damages considered. *Acta Mechanica Solida Sinica* 25:361-376. DOI: 10.1016/S0894-9166(12)60033-0
- Feng XT, Ding WX (2007) Experimental study of limestone micro-fracturing under a coupled stress, fluid flow and changing chemical environment. *International Journal of Rock Mechanics and Mining Sciences* 44:437-448. DOI: 10.1016/j.ijrmms.2006.07.012
- Grgic D, Giraud A (2014) The influence of different fluids on the static fatigue of a porous rock: Poro-mechanical coupling versus chemical effects. *Mechanics of Materials* 71: 34-51. DOI: 10.1016/j.mechmat.2013.06.011
- Chai ZY, Kang TH, Feng GR (2014) Effect of aqueous solution chemistry on the swelling of clayey rock. *Applied Clay Science* 93-94: 12-16. DOI: 10.1016/j.clay.2014.02.027
- Feng XT, Ding WX, Zhang DX (2009) Multi-crack interaction in limestone subject to stress and flow of chemical solutions. *International Journal of Rock Mechanics and Mining Sciences* 46: 159-171. DOI: 10.1016/j.ijrmms.2008.08.001
- Xu RN, Luo S, Jiang PX (2011) Pore scale numerical simulation of supercritical CO₂ injecting into porous media containing water. *Energy Procedia* 4: 4418-4424. DOI: 10.1016/j.egypro.2011.02.395
- Gao H, Li HZ (2015) Determination of movable fluid percentage and movable fluid porosity in ultra-low permeability sandstone using nuclear magnetic resonance (NMR) technique. *Journal of Petroleum Science and Engineering* 133: 258-267. DOI: 10.1016/j.petrol.2015.06.017
- Zargari S, Canter K.L, Prasad M (2015) Porosity evolution in oil-prone source rocks. *Fuel* 153: 110-117. DOI: 10.1016/j.fuel.2015.02.072
- Schoenfelder W, Gläser HR, Mitreiter I, et al. (2008) Two-dimensional NMR relaxometry study of pore space characteristics of carbonate rocks from a Permian aquifer. *Journal of Applied Geophysics* 65: 21-29. DOI: 10.1016/j.jappgeo.2008.03.005
- She AM, Yao W (2010) Probing the hydration of composite cement pastes containing fly ash and silica fume by proton NMR spin-lattice relaxation. *Science China Technological Sciences* 53: 1471-1476. DOI: 10.1007/s11431-010-3134-1
- Luo S, Xu RN, Huang XW (2011) Visualization experimental investigations of supercritical CO₂ inject into porous media with the fissure defect. *Energy Procedia* 4: 4411-4417. DOI: 10.1016/j.egypro.2011.02.394
- Webber JB, Corbett P, Semple KT, et al. (2013) An NMR study of porous rock and biochar containing organic material. *Microporous and Mesoporous Materials* 178: 94-98. DOI: 10.1016/j.micromeso.2013.04.004
- Liu HB, d'Eurydice MN, Obruchkov S, et al. (2014) Determining pore length scales and pore surface relaxivity of rock cores by internal magnetic fields modulation at 2 MHz NMR. *Journal of Magnetic Resonance* 246: 110-118. DOI: 10.1016/j.jmr.2014.07.005
- Yao YB, Liu DM, Xie SB (2014) Quantitative characterization of methane adsorption on coal using a low-field NMR relaxation method. *International Journal of Coal Geology* 131: 32-40. DOI: 10.1016/j.coal.2014.06.001
- Wang XX, Shen XD, Wang HL, et al. (2015) Nuclear magnetic resonance analysis of concrete-lined channel freeze-thaw damage. *Journal of the Ceramic Society of Japan* 123: 1-9. DOI: 10.2109/jcersj2.123.43
- Xiao LZ, Liao GZ, Deng F, et al. (2015) Development of an NMR system for down-hole porous rocks. *Microporous and Mesoporous Materials* 205: 16-20. DOI: 10.1016/j.micromeso.2014.09.024
- Martin CD (1993) *The strength of massive Lac du Bonnet granite around underground openings*. Ph. D. Thesis, University of Manitoba, Manitoba, Canada.
- Eberhardt E, Stimpson B, Stead D (1999) Effects of grain size on the initiation and propagation thresholds of stress-induced brittle fractures. *Rock Mechanics & Rock Engineering* 32(2):81-99. DOI: 10.1007/s006030050026
- Everitt RA, Lajtai EZ (2004) The influence of rock fabric on excavation damage in the Lac du Bonnet granite. *International Journal of Rock Mechanics and Mining Sciences* 41(8): 1277-1303. DOI: 10.1016/j.ijrmms.2004.09.013